Effects of applying EGR with split injection strategy on combustion performance and knock resistance in a spark assisted compression ignition (SACI) engine

Lei Zhou[a#], Kai Dong[a#], Jianxiong Hua[a], HaiqiaoWei[a*], RuiChen[a,b],Yiyong Han[a,c]

[a]State Key Laboratory of Engines, Tianjin University, Tianjin 300072, China

[b]Department of Aeronautical and Automotive Engineering, Loughborough University, LE113TU, United Kingdom

[c]Yuchai Machinery Co.,Ltd.

**Corresponding author: Haiqiao Wei*

Address: 92 Weijin Road, Nankai District, Tianjin, P. R. China

Tel.: +86-22-27402609

[#]These authors contributed equally to this work and should be considered co-first authors

Email: whq@tju.edu.cn

Submitted to **Applied Thermal Engineering**

Article type: Research Paper

Abstract

Spark assisted compression ignition (SACI) is a proven method for extending the load range and controlling the combustion phase of homogeneous charge compression ignition (HCCI) while maintaining high thermal efficiency. However, the occurrence of abnormal combustion, such as knock, limits the improvement of efficiency in SACI combustion. In this study, the effects of a coupling strategy, which combines internal/external exhaust gas recirculation (i & e-EGR) and split injection, on knock suppression in SACI mode were investigated in a high-compression-ratio, single-cylinder gasoline engine with a fully variable valve system. During the experiment, the mass of intake air remained constant while e-EGR was added. The results show that the coupling strategy combines the advantages of e-EGR and split injection, providing an effective method for resisting knock and improving engine efficiency. The results also demonstrate that applying e-EGR to SACI combustion significantly decreases the knock intensity by effectively reducing the in-cylinder temperature. In addition, the effect of split injection on knock suppression is related to the initial in-cylinder temperature and fuel stratification. With high initial in-cylinder temperature, the relationship between knock probability and split injection timing is non-monotonic. However, with low initial in-cylinder temperature, the capacity of resisting knock monotonically increases with the delay of secondary injection timing.

Keywords: SACI, knock, internal EGR, external EGR, split injection

1. Introduction

Homogeneous Charge Compression Ignition (HCCI) offers significant advantages in improving the brake thermal efficiency (η) and emission, and has attracted attentions of many researchers worldwide [1]. However, there are still challenges for HCCI, including the narrow load range and uncontrollable combustion phase. Intensive works have been carried out to extend the HCCI operating range, and strategies such as exhaust gas recirculation (EGR) [2, 3], split injection [4, 5] and intake boost strategies [6, 7] were proposed. In spite of all these efforts, the maximum indicated mean effective pressure (IMEP) of HCCI is still lower than 0.5 MPa [8, 9]. Moreover, HCCI remains a challenge in combustion controlling due to lack of a direct ignition timing (IT) control mechanism [10]. Many researchers [11-15] have found that the spark assisted compression ignition (SACI) mode is a potential way to expand the HCCI load and control the combustion phase by adjusting IT.

With the aim of studying the mechanism of the SACI mode, different methods have been adopted in the last few years [16] to study the mechanism of the SACI mode. The SACI combustion process sequence was recorded by Wang [8, 17] and Benajes et al. [18, 19] with the use of the transparent engine. The conclusion can be summarized as follows: once the injection event finishes, the spark plug discharge will take place and consequently initiate the ignition and flame propagation process, in which the energy release causes an increase of pressure and temperature in the unburned gas zone, finally leading to a second phase of combustion governed by the auto-ignition of the rest of the mixture**.** In addition, Lavoie et al. [20] delineated the regimes to compare the different combustion modes in a multi-mode combustion diagram in terms of unburned and burned gas temperatures near top dead center. The analysis on experimental data suggests that SACI combustion mode is very suitable for the high and moderate loads to obtain the best performance, but the η deteriorates as the load is reduced.

Additionally, in order to control the SACI combustion mode, different strategies have been proposed for adjusting the combustion phase and noise [9, 10, 21-24]. Many studies, including the experimental research of Olesky et al. [10] and numerical investigations by Robert. et al. [9], have also shown that the spark timing and in-cylinder temperature strongly affect SACI combustion phasing. The experimental results [10] show that the reduced peak of heat release rate (HRR) is achieved by controlling spark timing and unburned gas temperature with the fraction of flame heat release increased. The simulation results [9] show that the reduction in the peak HRR during the auto-ignition process is a function of both the end-gas mass and the end-gas reactivity. Another strategy deeply investigated by researchers is the split injection strategy [25]. Persson et al. [26] studied the SACI with ethanol as fuel in order to understand the effect of fuel stratification when using high speed fuel PLIF. The research result shows the occurrence of ignition in the mixing zone between the rich and the leaner regions. A parametric study was carried out by Benajes et al. [27], which was applied to the spark assisted partially premixed compression (PPC) ignition combustion mode under light load with the global lean equivalence ratio operating conditions. It was found that the split injection strategy can better realize the combustion phase control and improve combustion performance and emission performance compared with the single injection.

The above studies mainly emphasize on the mechanism of SACI combustion mode and the strategies of improving its performance. However, few researchers studied the knock phenomenon in SACI mode. The rapid auto-ignition of the end mixture can lead to the occurrence of knock phenomenon, thus limiting the increase of η and producing combustion noise under SACI mode with high load [21]. The e-EGR and stratified mixture are the effective strategies for suppressing knocking in GDI engines [28-30]. However, there are few literatures reflecting the use of higher compression ratio (CR), e-EGR coupling with stratified charge to realize SACI.

Therefore, the present work experimentally and systematically investigated the effects of a strategy of internal/external EGR coupling with split injection on combustion characteristics as well as knock suppression in a higher CR-GDI engine with a fully variable valve train (VVT). In particular, the impacts of the combined strategies on the pressure oscillation, knock intensity, HRR, in-cylinder temperature, η, etc. are systematically studied in this paper. The present work will give a valuable insight into the design of new engine.

The rest of this paper is organized as follows: section 2 describes the experimental facilities and operation conditions, as well as the evaluation methods for onset and intensity of SACI knock. Section 3 presents a detailed description of the effects on SACI combustion characteristic when e-EGR, split injection strategies, and e-EGR combined with split injection are adopted, respectively. Finally, the main conclusions of the study are presented in section 4.

2. Experiment study

2.1 Experimental setup

The engine used for this experiment was a Ricardo E6 4-stroke SI engine. Details of the engine specifications are provided in Table 1. A schematic view of the engine and instrumentation setup is shown in Fig. 1. The cylinder bore, stroke, and compression ratio (CR) are 80 mm, 100 mm, and 12:1, respectively. A double-spark ignition system was used in this study to guarantee stable combustion. The two spark plugs are symmetrically mounted on the cylinder head. The engine was equipped with a direct current dynamometer with a speed accuracy of ±0.2%. The in-cylinder pressure was measured by a pressure transducer (Kistler 6118B) mounted in the cylinder. The signal was then passed to a Kistler 5011 charge amplifier and finally to a National Instruments PC-612 data acquisition card. The equivalence ratio was measured by a wideband lambda sensor with a measurement accuracy and uncertainty of ±0.1% and ±0.8%, respectively, and a response time within 0.15 s. The SIEMENS Proportional

Integral Differential (PID) controller measured the coolant and oil temperatures with an uncertainty of ±3°C. All temperatures were measured with K-type thermocouples. The fuel injection system is based on an electronic control unit (MOTEC M400). To achieve split injection, a piezoelectric injector with a hollow-cone structure was used. Fuel mass was measured by a fuel consumption meter with an accuracy of ±0.5%. Figure 1 shows the relative position of the injector and the spark assembly in the cylinder head. This relative position combined with the tumble flow was fixed to make the spray pass between the spark electrodes.

Table 1. Engine specifications

Engine type	Single cylinder,4-stroke
Bore×stroke (mm)	80×100
Displacement (L)	0.5
Compression ratio	12:1
Valve mechanism	2-valve,VVT
Throttle	WOT
Piston shape	Flat
Fuel injection	Direct injection
Injection pressure(bar)	200
Fuel	Gasoline 92 RON
Equivalence ratio	1.0

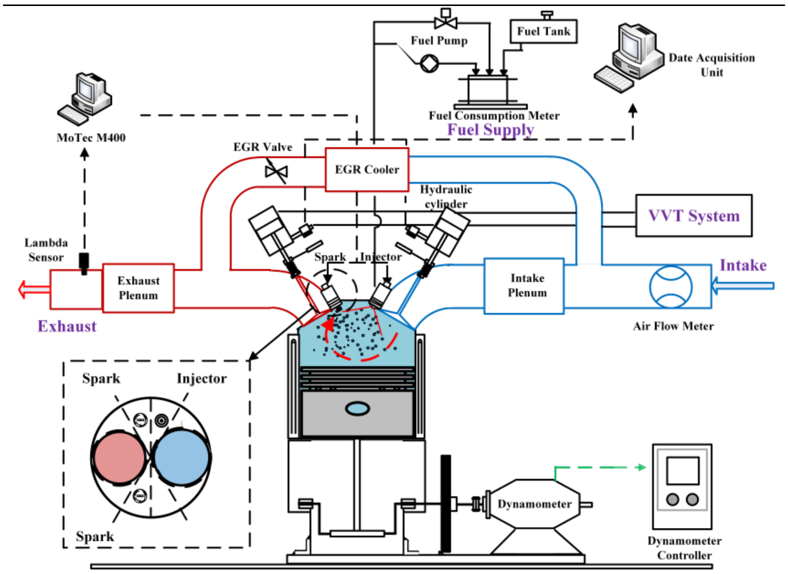

Fig. 1. Schematic view of the engine and instrumentation setup.

As shown in Fig. 2(a), another major feature added to the engine is a highly flexible electro-hydraulic valve train installed on both the intake and exhaust sides to achieve negative valve overlap (NVO). The engine also has an e-EGR loop. The valve lift curves for the basic measurements (i-EGR strategy) used in the experiments are shown in Fig. 2(b). Symmetric NVO operation with fixed exhaust valve closing (EVC) and intake valve opening (IVO) timing was used to retain high temperature, enabling the SACI combustion mode [9]. Throughout the experiments, the locations of intake valve closing (IVC) and exhaust valve opening (EVO) were held constant, enabling the effective compression ratio to remain fixed. The EGR ratio is calculated as follows in Eqs. (1), (2) and (3) [29, 31, 32].

$$m_{tot} = m_{fuel} + m_{air} + m_{e-EGR} + m_{i-EGR} \tag{1}$$

$$m_{i-EGR} = m_{tot}\left(\frac{V_{EVC}}{V_{EVO}}\right)\left(\frac{P_{EVC}}{P_{EVO}}\right)^{\frac{1}{\gamma}} \tag{2}$$

$$\left(m_{e-EGR} + m_{air}\right) * XO2_{man} = m_{air} * XO2_{amb} \tag{3}$$

where m_{tot} is the total mass of burned gas in the combustion chamber before EVO, m_{fuel} and m_{air} are measurements of the injected fuel mass and intake air mass, respectively. m_{e-EGR} is the mass of e-EGR, which can be acquired from CO_2 or O_2 measurements in the intake and exhaust pipes. $XO2_{amb}$ represents the concentration of oxygen in the environment, and $XO2_{man}$ represents the concentration of oxygen after the mixing of exhaust gas and intake fresh air measurements in the intake pipe. m_{i-EGR} is the internal residual mass and was estimated by several different methods. The Mirsky Method, which is sufficiently accurate and requires simple calculations, was proposed by Yun and Mirsky and is chosen for calculating i-EGR ratio [31]. γ represents the ratio of specific heats. The ratio of specific heats from EVO to EVC is estimated by taking the average of the γ values obtained using the temperatures at EVO and EVC. When calculating $m_{i\text{-}EGR}$, the value of 1.35 for γ is utilised taking into consideration of the existence of CO_2 and H_2O, which are the primary substances in EGR gases. Additionally, it was verified that the method of calculating $m_{i\text{-}EGR}$ is not sensitive to the γ, suggesting that the value selected in this paper is reasonable.

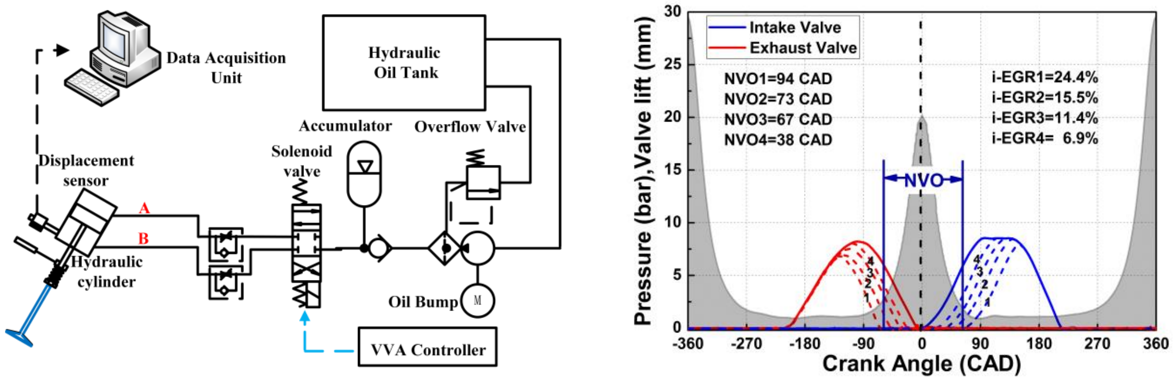

(a) Schematic of VVT System

(b) Schematic of valve lift profiles

Fig. 2. Schematic views of the VVT system and the valve lift profiles for different SACI modes.

2.2 Operation conditions

After warming up the engine, it operates with wide open throttle (WOT). Measurements were obtained at a constant engine speed of 1500 rpm with equivalence ratio of 1.0. The oil temperature was 85±3°C. The engine coolant temperature, which was controlled by the Siemens PID, was maintained at 75±3°C. The intake manifold temperature was 20±3°C. Atmospheric backpressure was used irrespective of the intake pressure. The fuel used in experiments was commercial petrol with research octane number of 92. Pressure signals were obtained with crank angle intervals of 0.1 CAD for 200 consecutive cycles. The basic measurements were as follows: a sweep of the symmetric NVOs, including 94 CAD, 73 CAD, 67 CAD, and 38 CAD, was conducted, corresponding to i-EGR ratios of 24.4%, 15.5%, 11.4%, and 6.9%, respectively. The injection control system makes it possible to modify any parameter of the injection event, like injection timing, duration and rail pressure. In this paper, the start of injection timing was set to be 300 CAD BTDC in order to obtain a homogeneous charge. A constant injection pressure of 200 bar was used for all measurements.

Table 2 shows the four groups of operating conditions studied in this paper. Group 1 aims to study the effects of i-EGR ratios, which is realised by various NVOs with a single injection and no e-EGR. Group 2 combines the i-EGR and e-EGR strategies, and intake mass flow rate and fuel mass per cycle are held constant. This is achieved by simultaneously adjusting the e-EGR valve and NVO. Group 3 is designed to study the effects of split injection strategies on knock suppression and engine performance. Finally, the combination of internal/external EGR strategies and split injection strategy are utilised to extract better engine performance and fuel economy.

Table 2. Operating conditions for the different strategies.

Inject Strategy	SOI$_1$ (CAD BTDC)	SOI$_2$ (CAD BTDC)	ROI$_1$: ROI$_2$	Intake XO2(%)	i-EGR (%)	e-EGR (%)	Fuel mass (mg)
Single	300	\	\	21	24.4	\	23.5
					15.5		28.7
					11.4		32.0
					6.9		36.1
Single	300	\	\	20	13.9	3.9	28.7

				19	12.1	7.9	
				18	10.4	12.2	
				17	7.0	18.2	
					24.4		23.5
Split	300	180-60	4:1	21	15.5	\	28.7
					6.9		36.1
Split	300	180-60	4:1	17	7.0	18.2	28.7

2.3 Evaluation methods for onset and intensity of SACI knock

As reported in many previous studies, knocking combustion generates high frequency in-cylinder pressure oscillations ranging from 4 kHz–20 kHz [33, 34]. Therefore, a band-pass filter of 4 kHz–20 kHz is used to extract the pressure oscillations from the original in-cylinder pressure signal. According to Nyquist sampling theorem, the highest frequency component that can be analysed is one-half the sampling frequency. Under the conditions of the experiment, the sampling frequency is 90 kHz, which is sufficient to capture the knocking signal in the region of 4 kHz–20 kHz. To quantify the intensity of engine knock, the maximum amplitude of filtered pressure oscillation (MAPO), which is calculated from filtered pressure, has been used as the knock indicator in this study. This indicator directly reflects the pressure fluctuation amplitude of knock combustion [35].

Statistical analysis is conducted to distinguish the conditions of normal combustion, critical knock and heavy knock under the SACI combustion mode, which is shown in fig. 3. In the experiment, no knocking sound was heard under the conditions of normal combustion. A slight knocking sound was heard under critical knocking conditions, and a sharp knocking sound was heard when heavy knocking occurred. In the fig. 4, with ITs during 4-10 CAD BTDC, no clear increases in the average MAPO can be observed. However, when the ITs change from 10 CAD BTDC to 14 CAD BTDC, the average MAPO clearly rises. Therefore, a MAPO value of 0.2 MPa was selected as the knock threshold for the critical knock condition. If the MAPO of an individual combustion cycle exceeds this threshold, it is regarded as a knocking cycle. Furthermore, if the knocking cycle exceeds 10% for a given operating condition, it is also considered a knocking condition [36]. Based on this methodology, the conditions of normal combustion, critical knock and heavy knock can be well distinguished.

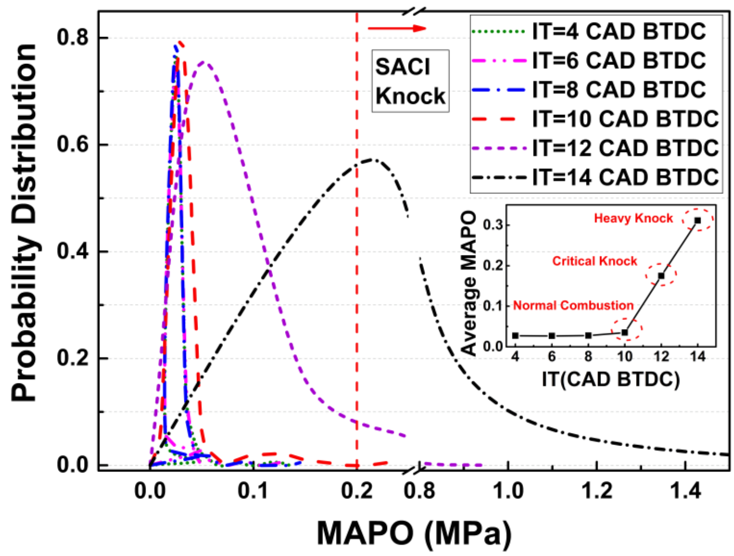

Fig. 3. Probability distribution of MAPO under SACI combustion mode.

Figure 4 compares the normal and knocking combustion process of the SI and SACI modes. The pressures, pressure oscillations and HRRs are shown in Fig. 4. Note that the two combustion modes (SI and SACI) have the same control parameters (e.g., compression ratio, intake mass flow rate, fuel amount, equivalence ratio). When knock occurs, the knocking sound can be heard in both SI and SACI combustion. In the case of the SACI, the throttle was widely opened and the intake mass flow was adjusted by the NVO, while that of the SI conditions was controlled by the throttle open degree. Therefore, the in-cylinder pressure and temperature of the SACI before combustion are higher than those of the SI mode. Due to the higher initial temperature and pressure of the SACI, more fuel is involved in auto-ignition, which leads to a faster burning rate and more intensive pressure oscillations than in SI combustion. In other words, the knock intensity of the SACI is generally higher than that of the SI. Additionally, the dashed lines show the normal conditions of combustion for the SACI and the SI. The HRR of the SI is low and smooth, while the HRR of the SACI has an obvious inflection point, which is the point at which auto-ignition occurs. Because of the effects of CO_2 and H_2O with regard to dilution and heat capacity, such auto-ignition is controllable and does not result in an intensive combustion process. Consequently, this controllable auto-ignition helps to improve engine performance.

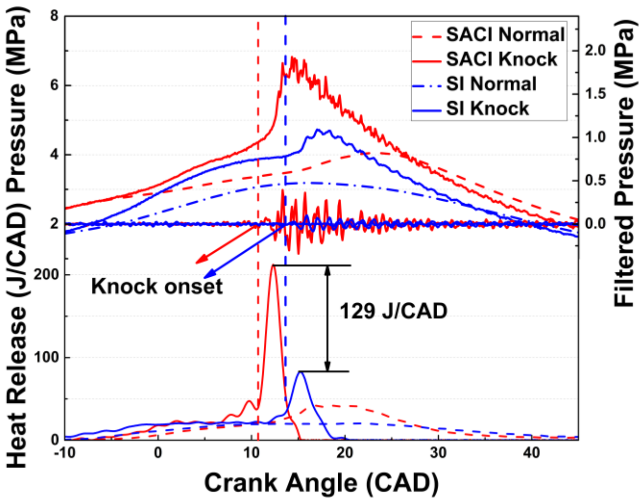

Fig. 4. Comparison of knock phenomena under SACI and SI combustion modes.

3. Results and discussion

3.1 Combustion characteristics with i-EGR (i-EGR strategy)

In this section to facilitate the analysis and comparison, preliminary results of tests using only i-EGR and single injection strategy will be presented. By understanding the influences of

IT and i-EGR on SACI combustion mode, further research can be carried out on optimisation by means of other strategies.

In this paper, the ratio of the amount of fuel consumed by flame propagation (SI combustion) is defined as R_{si}. The auto-ignition timing of the unburned gas is defined as the first maximum point of the second derivative of the HRR ($d^2HRR/d^2\varphi$) [37, 38]. The value of R_{si} is equal to the MFB value at the point of auto-ignition timing. The ratio of fuel consumed by the CI process, R_{ci}, is equal to 1-R_{si}.

Figure 5(a) illustrates the effects of different ITs on in-cylinder pressure, HRRs and mass fraction burned (MFB) with an i-EGR ratio of 24.4% in the SACI combustion mode. It can be observed that the peak pressure increases and advances while advancing the IT. Meanwhile, a faster burning rate and shorter combustion duration can be obtained due to the earlier onset of combustion. When advancing IT, R_{ci} increases, exhibiting a higher HRR peak. This is because advancing the IT can lead to higher in-cylinder combustion temperature and pressure, and the ignition delay time of the unburned mixture decreases, thus leading to earlier auto-ignition during the experiment, which prompts more fuel to participate in the second stage of the compression ignition process. These effects lead to the CI process being overly violent and generating strong pressure oscillations in the cylinder. Note that, as the IT is significantly delayed, the heat release process gradually gets closer to that of the SI mode, and misfire cycles occasionally appear during the experiments. This is because the combustion phase is delayed when IT is delayed, and the combustion temperature and pressure in the cylinder are not sufficiently large to cause auto-ignition of the unburned gas. In addition, the larger i-EGR rate reduces the stability of combustion. These results indicate that IT is a key parameter in controlling the SACI combustion process. It can be found that, with appropriate i-EGR, the combustion mode can be transitioned from SI to SACI by advancing the ITs [8]. It is important to note that, when ignition is too early, it causes SACI knock.

Figure 5(b) illustrates the in-cylinder pressures, HRRs and MFBs of the minimum spark advance for best torque (MBT) conditions at different i-EGR ratios. The MBT conditions are determined by IT sweeps at each i-EGR ratio. As shown in Fig. 5(b), as the i-EGR ratio decreases, the peak HRR increases gradually while the peak pressure drops slightly. Due to the stoichiometric combustion in SACI, the decrease in i-EGR results in more fuel being injected into combustion chamber, which increases engine load. To avoid knock when load rises, the IT should be retarded, which slows the burn rate and lengthen the duration of combustion. Thus, the decline in peak pressure can be observed as the i-EGR decreases. In addition, the decrease in i-EGR results in an increase in R_{si}, which is due to the lower initial in-cylinder temperature and longer ignition delay of the unburned gas caused by the retardation of the IT. Therefore, a larger fraction of flame heat release is required to provide the additional compression heating needed for auto-ignition. When the i-EGR is insufficient, the auto-ignition process in the SACI mode diminishes due to the initial temperature being lower than the critical value. As a result, the combustion transitions from the two-stage SACI combustion mode to a single-stage traditional SI combustion mode. These indicate that i-EGR controls the combustion process of the SACI mode mainly by controlling the initial in-cylinder temperature and ambient gas components in the combustion chamber.

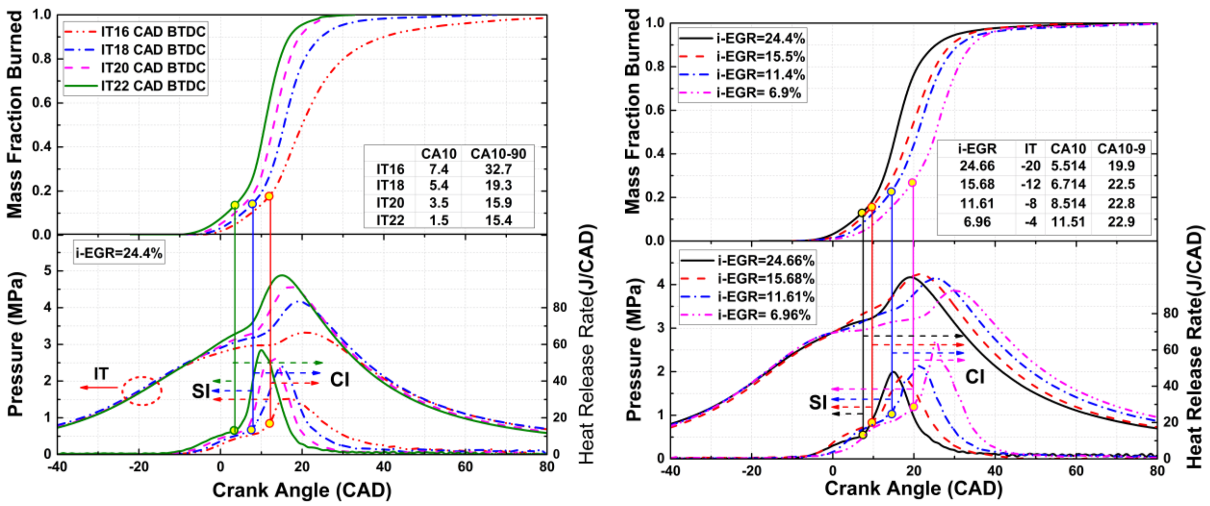

(a) Ignition timing variation　　　　(b) i-EGR rates variation

Fig. 5. SACI pressure, heat release, mass fraction burned under different ignition timing and i-EGR rates.

Figure 6 shows the brake mean effective pressure (BMEP) and brake specific fuel consumption (BSFC) achieved over the region of stable combustion of the SACI engine in this experiment. As the i-EGR increases, the air/fuel mixture becomes more diluted, which requires advanced IT to maintain combustion stability. It can be observed from Fig. 6(a) that the stable combustion region of SACI can be made relatively wide by changing the i-EGR ratio and the IT. The area beyond the stable region is the knocking region, in which the IT is relatively advanced at a certain i-EGR ratio. Conversely, the area below the stable region is the instable combustion region, in which the i-EGR ratio is relatively large and the IT is relatively retarded. Meanwhile, the corresponding BSFC varies from 236 g/kW·h to 242.8 g/kW·h at the MBT point, as shown in Fig. 6(b). At high load conditions, the operating range is relatively narrow and the BSFC is slightly higher relative to those at the other conditions.

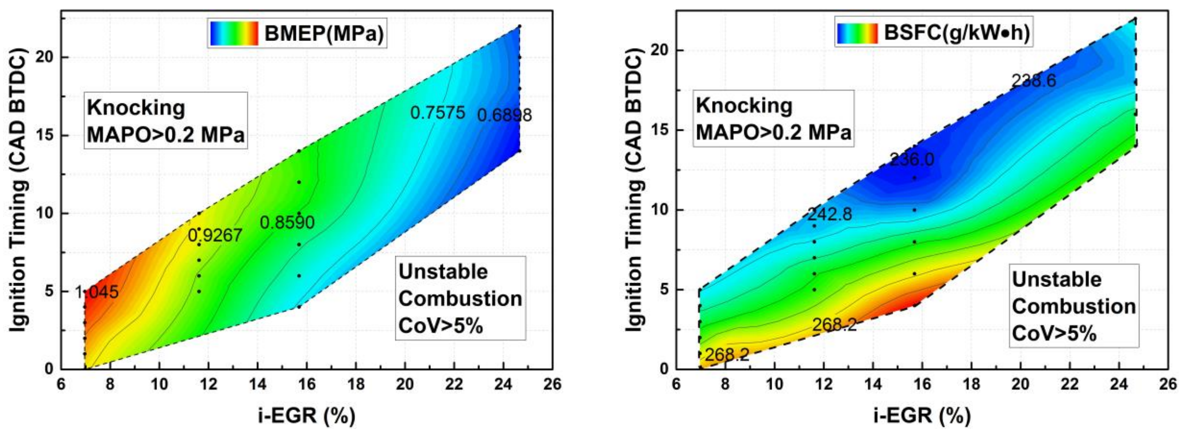

(a) BMEP of SACI

(b) BSFC of SACI

Fig. 6. BMEP and BFSC achieved over the region of stable SACI combustion at the stoichiometric condition.

It can be seen from above results that both ITs and i-EGR are effective methodologies for controlling the combustion phase of SACI. However, when the auto-ignition exceeds the buffer capacity of the inert gas, a strong pressure oscillation occurs in the cylinder, leading to a deterioration of thermal efficiency and fuel economy. Therefore, knock in the SACI mode is an important issue that limits the η. This phenomenon warrants further investigation.

3.2 Combination of internal and external EGR (i & e-EGR strategy)

In this section, the effects of a combined strategy utilising both internal and external EGR (i & e-EGR) on knock suppression and engine performance will be presented. The intake mass flow rate and fuel injection mass are held constant at 17.8 kg/h and 28.7 mg/cycle, respectively. When e-EGR is introduced into combustion chamber, the negative valve overlap (NVO) must be adjusted to ensure constant intake mass flow rate. O_2 concentrations (XO2) between 21%–17% are tested in this experiment, with the no e-EGR (XO2=21%) condition designated as the baseline case.

Figure 7 shows the MAPO distributions and the average MAPO over 200 consecutive cycles with different amounts of intake XO2 at IT=14 CAD BTDC. When the MAPO is greater than 0.2 MPa, the cycle is considered to be a knock cycle. As seen from the MAPO distributions, as the intake XO2 is gradually decreased, the knocking cycles gradually disappear and the amplitude of the pressure oscillations significantly decrease. As can be seen from the average MAPO, the average MAPO variation that results from adjusting the ratio of i-EGR to e-EGR is not significant, though the IT clearly advances. These results indicate that the i & e-EGR strategy could further suppress knock compared to the i-EGR strategy. The larger the ratio of e-EGR, the stronger the effect on knock suppression can be achieved. It is primarily the introduction of e-EGR that reduces the burning rate and the temperature in the combustion chamber, which is shown in Fig. 8.

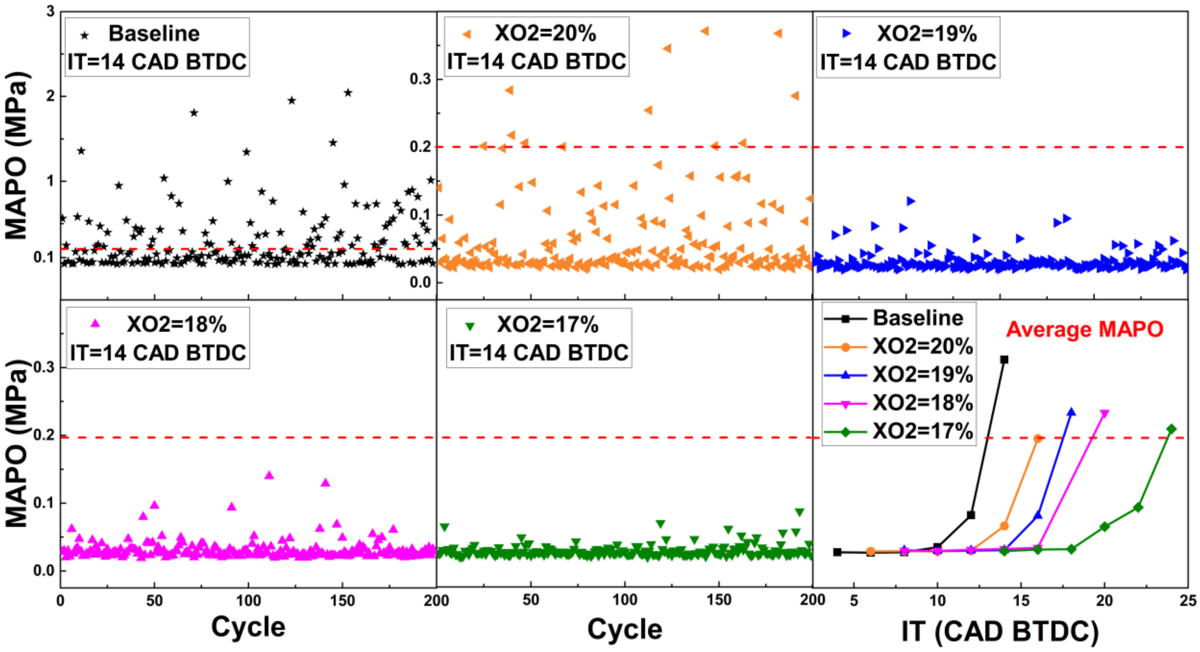

Fig. 7. MAPO distributions and the average MAPO for the baseline and i & e-EGR strategies.

Figure 8 shows the HRRs, MFBs and unburned temperature at different e-EGR ratios. In this study, the burned and unburned temperatures were calculated using a two-zone model [39, 40]. The calculation was performed using GT-Power software based on actual pressure data collected from the experiments. As shown in Fig. 8(a), under the same operating conditions, there is an obvious pressure oscillation in the baseline case. In the baseline case, the initial in-cylinder temperature is relatively higher (Fig. 8(b)), leading to a decrease in the ignition delay time of the unburned mixture. By introducing a large amount of e-EGR, the burning rate reduces and the combustion duration is prolonged since both the SI and CI combustion stages are suppressed [8]. These phenomena lead to a decrease in the R_{ci} and the pressure oscillation, thereby suppressing knock. This is because the initial in-cylinder temperature decreases with the addition of external cooling EGR. At the same time, due to the gas expansion and contraction characteristics, the total EGR in combustion chamber increases for further diluting the fuel/air mixture. Consequently, more fuel participates in flame propagation and less fuel participates in auto-ignition. . Therefore, the value of R_{ci} in the baseline case is the largest and the combustion duration is the shortest compared to the other cases. This indicates that the effects of e-EGR on knock suppression are generally achieved by decreasing the initial in-cylinder temperature and lengthening the ignition delay time of the unburned mixture, due to the effects of dilution and heat capacity changing on the existence of CO_2 and H_2O.

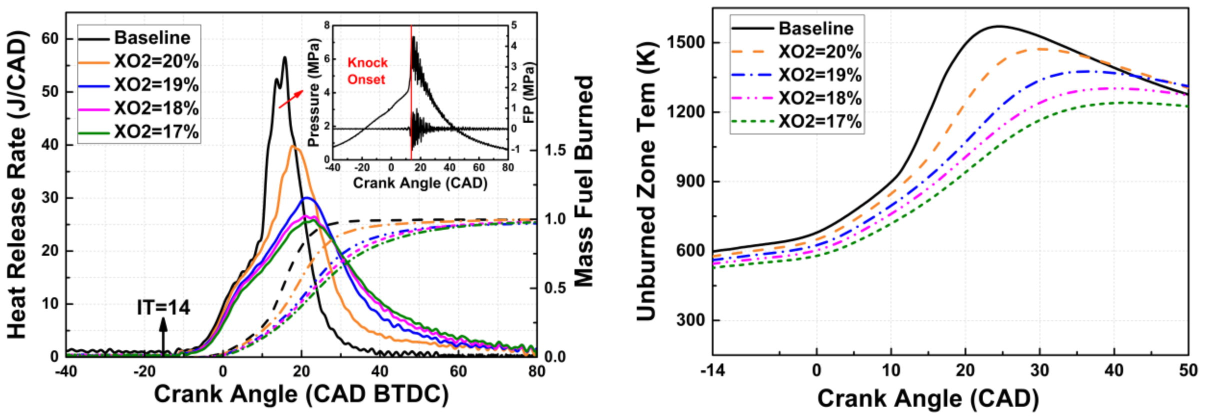

(a) Heat release rate and mass fraction burned (b) Unburned zone temperature

Fig. 8. Comparison of combustion characteristics between the baseline and i & e-EGR strategies.

In addition to the knock-suppressing effect, the addition of e-EGR is effective in improving engine performance. Figure 9 shows the BMEP and BSFC at different ITs for the baseline case and the cases with varying i & e-EGR strategies. As shown in Fig. 9, on the left of the red vertical dashed line (the MBT point of the baseline case), the BMEP declines and BSFC increases with the addition of e-EGR at the same IT. After the baseline case reaches the MBT point, further increase in IT leads to knock and a decrease in power output. As the e-EGR ratio is gradually increased, the engine's capacity for knock resistance increases, allowing more advanced ITs and higher BMEP to be achieved. The improvement in BMEP comes from two factors—optimisation of the combustion process and lower compression work during the NVO. As shown in the P-V diagram, the maximum in-cylinder pressure of XO2=17% with IT=22 CAD BTDC is significantly higher than that at the MBT point of the baseline case, which results in higher output work ($work^{+}$, 20.9 J improvement). This is mainly because a faster burning rate can be achieved by advancing IT. On the other hand, when a greater amount of e-EGR is introduced into combustion chamber, the NVO must be narrowed, which reduces negative work and heat dissipation during re-compression of the residual gas. The negative work (work$^-$) generated during the NVO reduces by 13.3 J, as shown in the P-V diagram in Fig. 9. Essentially, more advanced IT and less negative work during the NVO period can be achieved to optimise the combustion phase and engine performance, which leads to improved fuel economy.

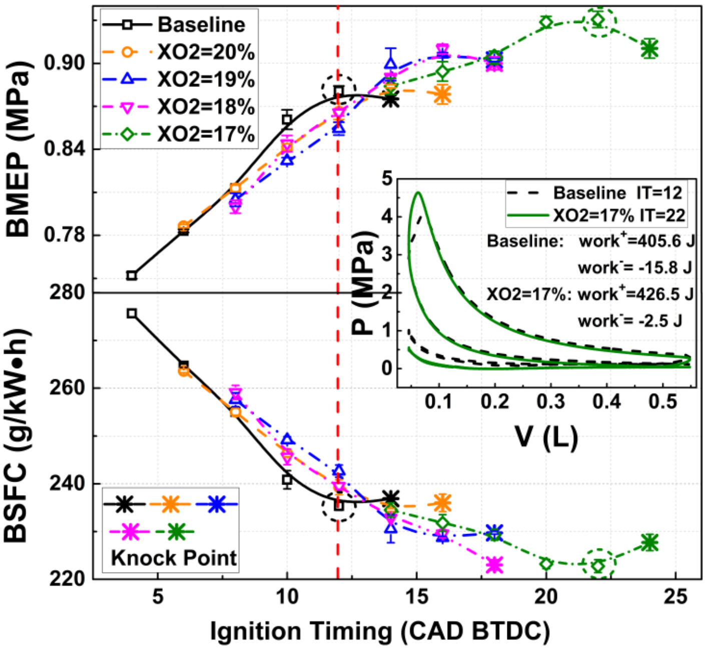

Fig. 9. BMEP and BSFC results for the baseline and i & e-EGR strategies ("work+" represent the positive work generated during compression stroke and power stroke; "work-" represent the negative work generated during exhaust stroke and intake stroke).

3.3 Combination of internal EGR and split injection (i-EGR & Split strategy)

In this section, the effects of a combined strategy utilising i-EGR and split injection (i-EGR & Split strategy) on knock suppression and engine performance are analysed. The start of the first and second injection timings are denoted SOI_1 and SOI_2, respectively. SOI_1 is set at 300 CAD BTDC, similar to that of the i-EGR strategy, to ensure sufficient mixing time for fuel injected by SOI_1, which allows for the formation of a homogeneous charge. Setting SOI_2 to occur during the compression stroke can produce a weak stratified charge based on the first injection [41]. The split ratios of SOI_1 and SOI_2 were set to be 4:1 in this section, which corresponds the optimised split ratio determined by the experiment shown in Fig. 10. At the MBT points of the different split ratios with an i-EGR ratio of 15.5%, it is clear that the best choice of split ratio is 4:1, which exhibits the highest BMEP. During the experiment, the cases applying only i-EGR strategies with i-EGR rates of 6.9%, 15.5%, and 24.4% are designated as baseline cases. A sweep of the SOI_2 from 180 CAD BTDC to 60 CAD BTDC in intervals of 40 CAD is utilised, with the i-EGR=15.5% case being chosen as the example to analyse the effects of SOI_2 on knock suppression and engine performance.

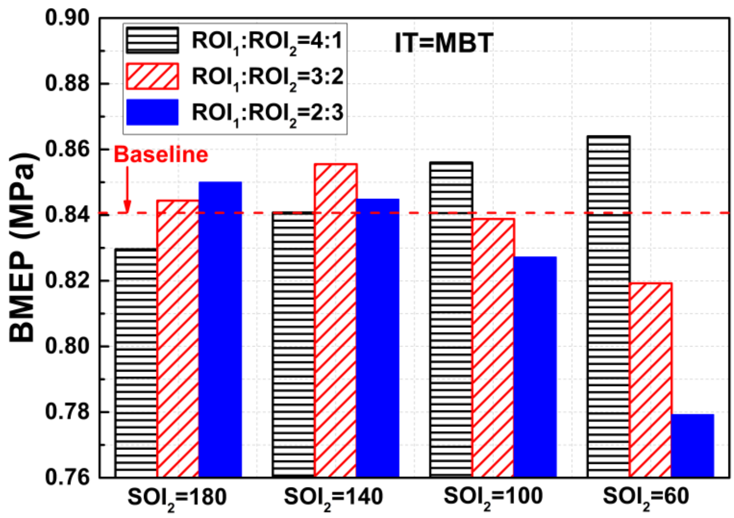

Fig. 10. BMEP with various split injection ratios of SOI_1 and SOI_2

Figure 11 illustrates the probability distribution of the MAPO with varying SOI_2 and ITs. It can be seen that, with a proper SOI_2, the probability distribution of the MAPO is more concentrated in the lower range compared to that of the baseline case. In SACI mode, as the IT advanced, the percentage of knock cycles gradually increased, and the MAPO distribution became more dispersed. Few or no knock cycles occurred at values of IT corresponding to 8-10 CAD BTDC. When the IT was set to a value of 12-14 CAD BTDC, the MAPO probability distribution gradually exceeded the knock critical value, and the percentages of knock cycles at all operating conditions increased. However, except for the case with SOI2=60 CAD BTDC, in which more knocking cycles occurred than that of baseline case at IT=14 CAD BTDC, the cases with SOI_2 between 180 CAD BTDC to 100 CAD BTDC show a good potential for suppressing knock. These latter cases exhibit lower percentages of knocking cycles than the baseline conditions. This is due to different split injection strategies forming different types of fuel stratification in cylinder. The equivalence ratio being developed in different areas in combustion chamber influences the flame propagation process and the later auto-ignition process. Overall, the results indicate that knock can be effectively suppressed by split injection with appropriate second-injection timings.

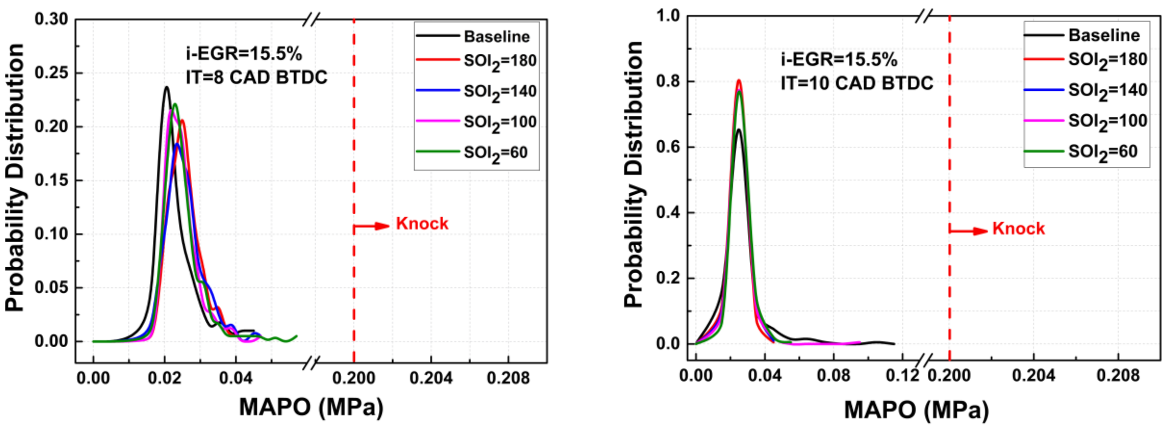

(a) IT at 8 CAD BTDC

(b) IT at 10 CAD BTDC

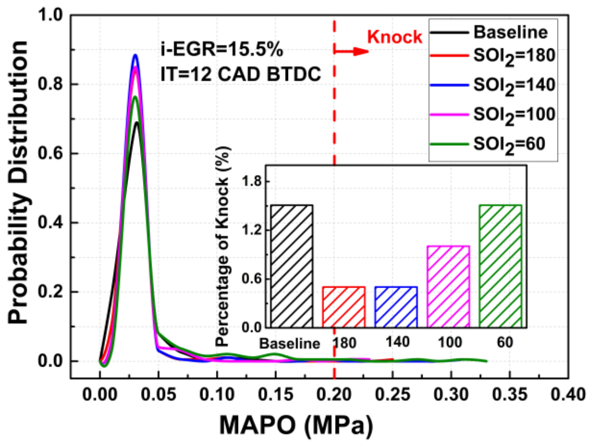

(c) IT at 12 CAD BTDC

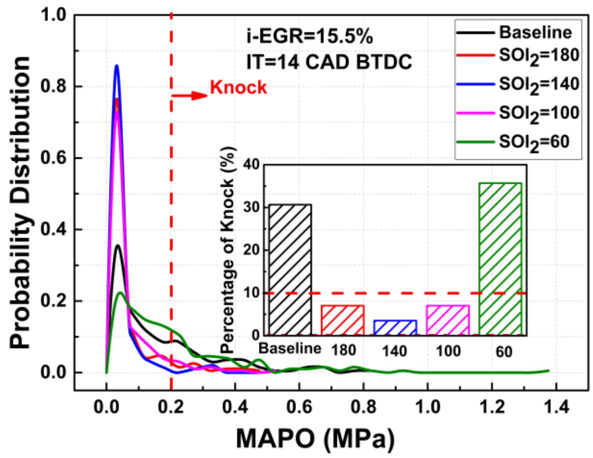

(d) IT at 14 CAD BTDC

Fig. 11. Knock probability distribution of baseline and i-EGR & Split strategy at different SOI$_2$.

Knocking sound could clearly be heard during the experiment when the IT is fixed at 14 CAD BTDC in the baseline case. Thus, the effects of split injection on knock resistance are analysed with IT=14 CAD BTDC. Figure 12 shows a comparison of the different combustion characteristics obtained using single injection and split injection strategies. As shown in Fig. 12(a), moving from the baseline case to the SOI$_2$=180-140 CAD BTDC cases, the peak HRR dropped as the combustion duration increased. This is because split injection can reduce the temperature around the spark plug via a cooling effect from the evaporation of local rich fuel (λ<1) [42]. Simultaneously, a lean fuel/air mixture is generated (λ>1) near the cylinder wall, which prolongs the ignition delay time of the unburned mixture. These two effects cause more fuel to participate in early flame propagation and reduce the proportion of auto-ignition. Consequently, the peak HRR gradually decreases and the combustion duration increases.

It should be emphasised that when the SOI$_2$ is retarded to 60 CAD BTDC, the peak HRR rises substantially with a decrease in combustion duration. The level of stratification is promoted by further retarding the secondary injection timing. At this point, the fuel/air mixture in the region of near the cylinder wall becomes leaner, which leads to a higher temperature in this region due to the attenuated cooling effect by fuel evaporation. The unburned zone temperature in Fig. 12(b) demonstrates the weaker cooling effect of fuel evaporation at the case of SOI_2 = 60 CAD BTDC compared with cases of SOI_2=180 CAD BTDC-100 CAD BTDC. Under the effect of the heat produced by i-EGR and the compression of flame propagation, the ignition delay time of the unburned mixture is shortened, which results in an earlier auto-ignition and a larger percentage of knocking cycles. These results indicate that the ability of the i-EGR & Split strategy to suppress knock in the SACI mode is affected by the level of fuel stratification. Moreover, the relationship between knock probability and SOI_2 is non-monotonic.

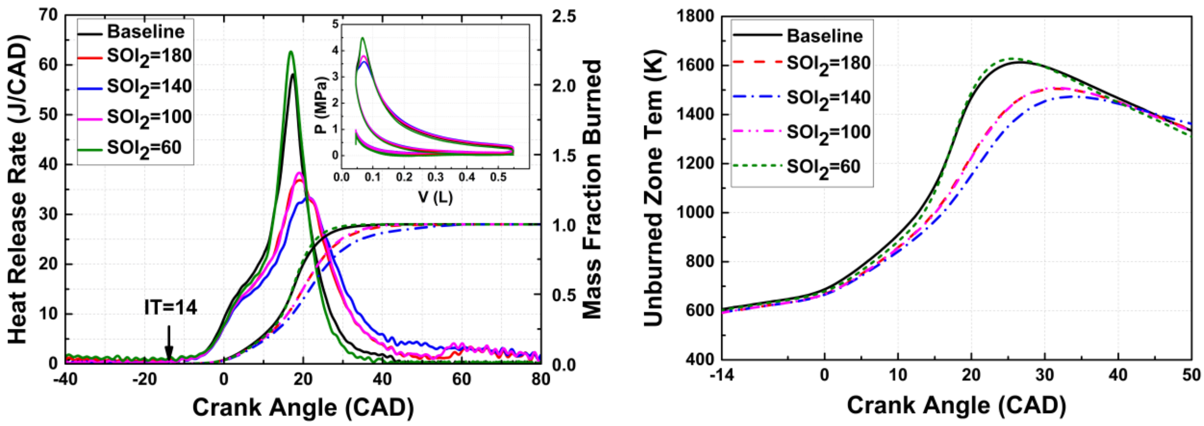

(a) Heat release rate and mass fraction burned (b) Unburned zone temperature

Fig. 12. Comparison of combustion characteristics among the i-EGR strategy and i-EGR & Split strategy at i-EGR=15.5%.

Figure 13 shows the effects of varying SOI_2 on knock suppression at different i-EGR rates.

It can be seen from Fig. 13 that in the cases of i-EGR=24.4% and i-EGR=15.5%, the ability of the split injection strategy to suppress knock first increases and then attenuates with the delay of SOI_2. However, when the i-EGR ratio is 6.9%, the knock suppression effect gradually increases as the SOI_2 is delayed. This is because the initial in-cylinder temperature is higher when i-EGR=24.4% and i-EGR=15.5%, and the later auto-ignition stage is more sensitive to the heat release of the early flame propagation stage. However, when i-EGR=6.9%, the later auto-ignition stage is less sensitive to the heat release of the early flame propagation stage due to a lower initial in-cylinder temperature. Overall, in SACI mode, the effect of knock suppression by the split injection strategy is also influenced by the initial in-cylinder temperature.

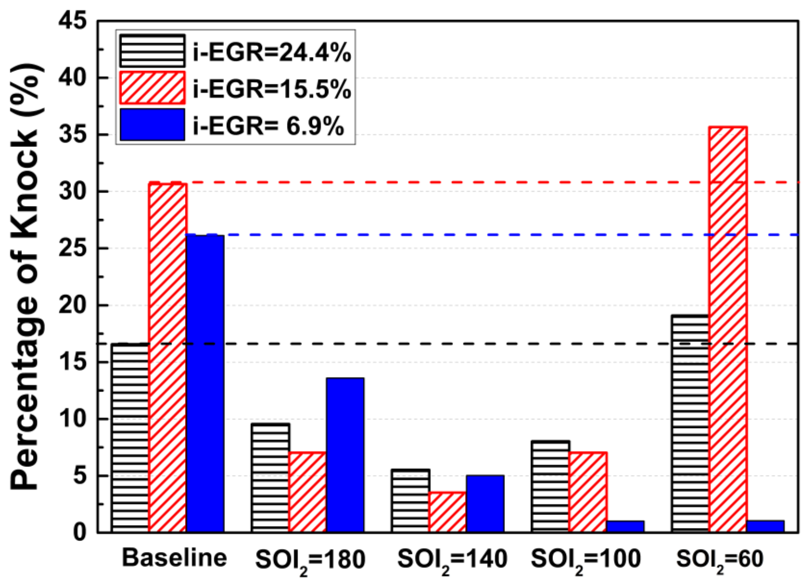

Fig. 13. Knock tendency of i-EGR & Split strategy at different i-EGR rates.

Figure 14 illustrates the BMEP and BSFC of the single injection strategy and the split injection strategy at the MBT point at different i-EGR ratios. It can be observed, from Fig. 14(b), that the BMEP of the MBT point with split injection are greater than those of the baseline case. As noted in Fig. 13, when i-EGR=24.4% and i-EGR=15.5%, a value of SOI_2=140 CAD BTDC corresponds to the best split strategy with regard to knock resistance. However, the best split injection strategy should produce the best BMEP while maintaining acceptable knock intensity. With this in mind, the best split injection strategies occur when both the knock resistance and power output are considered. As shown in Figs. 13 and 14(a), these optimal split injection strategies correspond to SOI_2=180 CAD BTDC, IT=20 CAD BTDC with i-EGR=24.4%, and SOI_2=60 CAD BTDC, IT=12 CAD BTDC with i-EGR=15.5%. It shows that the split injection strategy can directly influence the mixture formation process and, therefore, that it can produce changes in the combustion process. As a result, the secondary injection timing with the best knock suppression and that with the optimal power output are not necessarily in common. Figure 14(b) shows that BSFC of the i-EGR & Split strategy decreases by approximately 4.06 g/kW·h to 7.18 g/kW·h, which represents a significant improvement relative to the baseline.

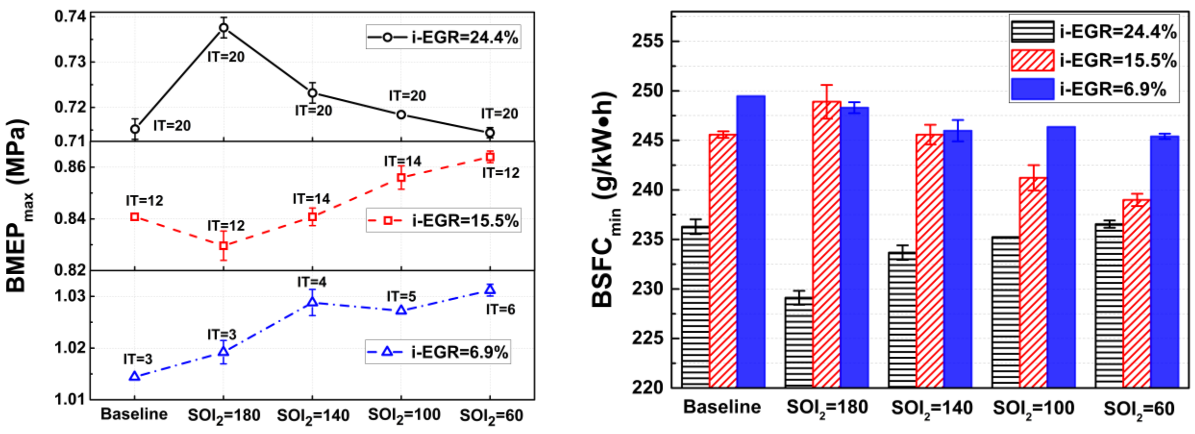

(a) BMEP　　　　　　　　(b) BSFC

Fig. 14. BMEP and BSFC for the i-EGR strategy and i-EGR & Split strategy at different loads.

3.4 Coupling strategies for internal/external EGR and split injection (EGR & Split strategy)

This section presents an analysis of the effects of a coupling strategy, which couples internal/external EGR and split injection (EGR & Split strategy), on knock suppression and performance optimisation in SACI mode. In this study, the fuel mass was maintained at 28.7 mg/cycle. At different operating conditions, the cases with the best anti-knock performance by adopting the optimal e-EGR ratio and SOI_2 were selected to perform a comparison. Based on the results from the previous sections, the optimal secondary injection timing for the i-EGR & Split strategy and the optimal e-EGR ratio for the i & e-EGR strategy are 140 CAD BTDC and XO2=17%, respectively. The strategy with XO2=17% and SOI_2=100 CAD BTDC is selected for the study of the EGR & Split strategy.

Figure 15 shows a comparison of the pressure and filtered pressure in the SACI mode for different strategies, including the i-EGR strategy, the i-EGR & Split strategy, the i & e-EGR strategy, and EGR & Split strategy. Figure 16 illustrates the percentage of knocking cycles and the maximum pressure in SACI mode for different strategies. From Fig. 15 and Fig. 16, it can be seen that the knock tendency of the baseline case is higher than that of any other cases, with the MAPO reaching approximately 1 MPa and the percentage of knock cycles reaching 30.7%. The MAPO and percentage of knocking cycles for the i-EGR & Split strategy are approximately 0.2 MPa and 3.5%, respectively. On the other hand, the MAPO is relatively low and no knocking cycles occur with the i & e-EGR strategy. These results imply that the e-EGR possesses superior anti-knock performance than split injection in SACI mode. In addition, the

EGR & Split coupling strategy combines the advantages of the e-EGR and split injection strategies and achieves the best performance with respect to knocking suppression.

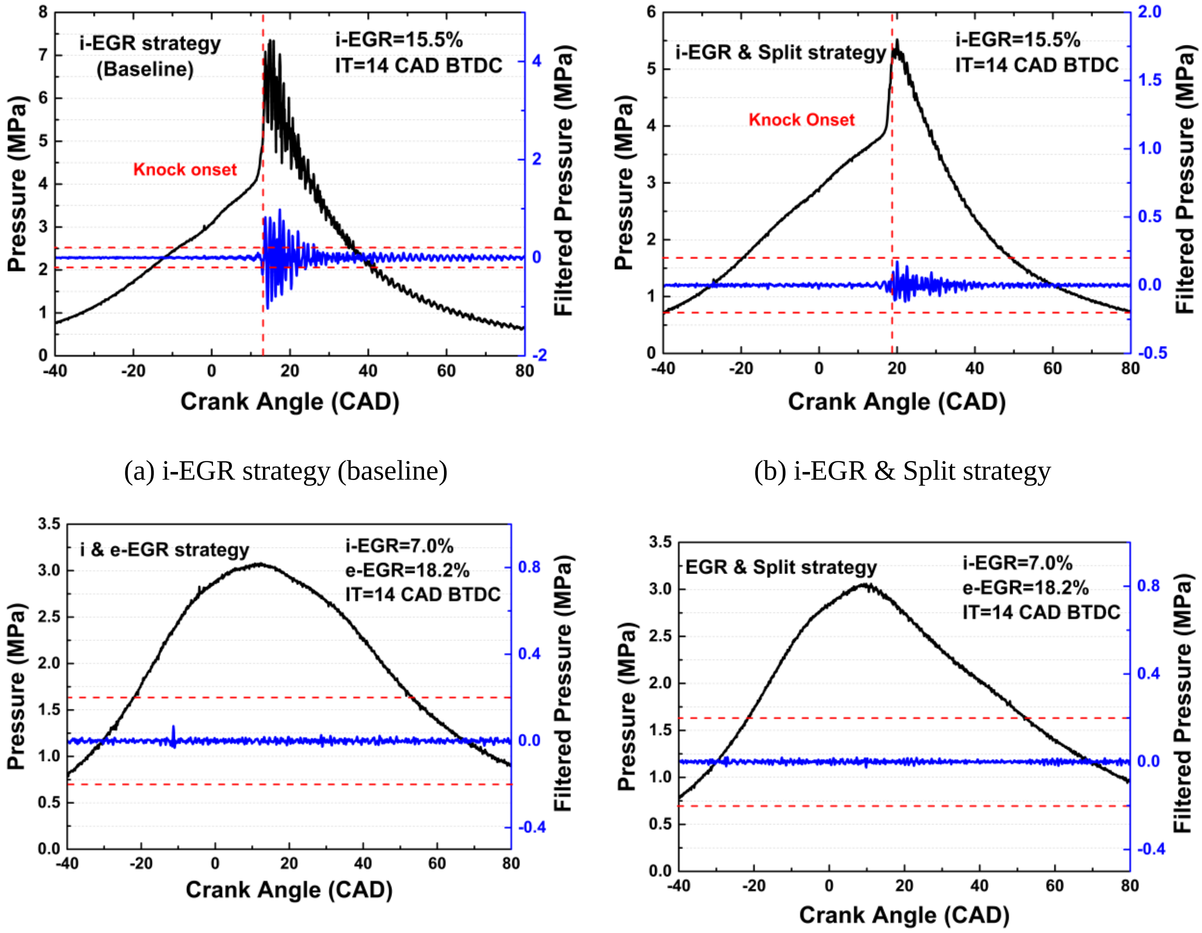

(a) i-EGR strategy (baseline)

(b) i-EGR & Split strategy

(c) i & e-EGR strategy

(d) EGR & Split strategy

Fig. 15. Pressure and filtered pressure in SACI mode with different strategies (EGR & Split strategy, which includes the i-EGR, e-EGR and split injection strategies).

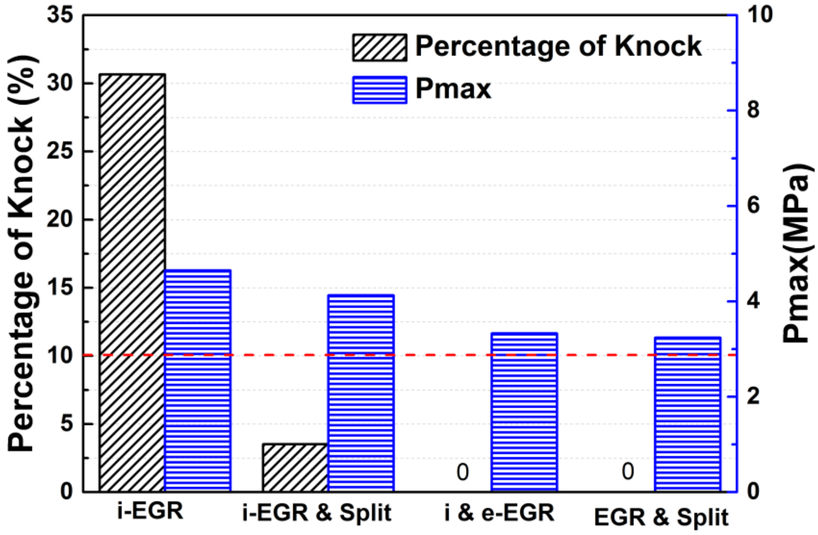

Fig. 16. Percentage of knock cycles and P_{max} in SACI mode with different strategies.

Figure 17 shows the BMEP and BSFC of the MBT points for different coupling strategies. It can be seen from Fig. 17 that the BMEP and BSFC of the coupling strategies were optimised relative to the baseline. This indicates that the coupling strategy considerably improves the combustion characteristics of the SACI mode by suppressing knock. However, the power output and fuel economy characteristics produced by the i & e-EGR strategy are higher than those produced by the i-EGR & Split strategy. This is mainly because, when the i & e-EGR strategy is used, the combustion phase can be optimised by applying a more advanced IT method on account of its better knock resistance. Based on this, the proposed EGR & Split strategy combines the advantages of i & e-EGR and split injection, which provides it the best combustion performance and an increase of approximately 0.1 MPa in the BMEP and a decrease of approximately 27 g/kW•h in the BSFC, relative to the baseline.

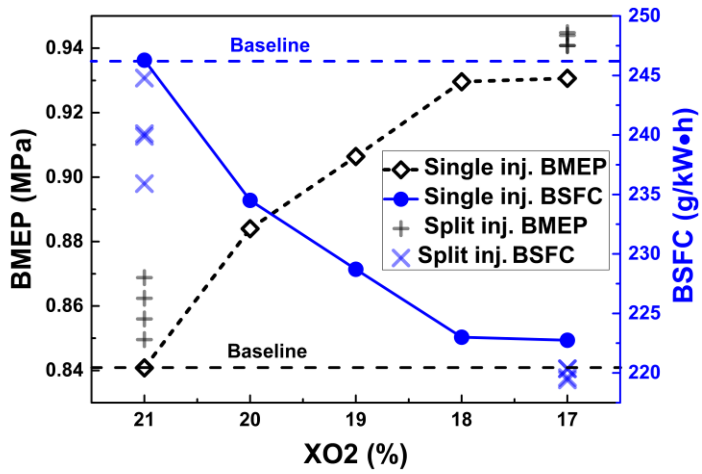

Fig. 17. BMEPs and BSFCs results for the different coupling strategies (where the x-coordinate represents the oxygen concentration, corresponding to different EGR strategies at different oxygen concentrations, and inj. denotes injection).

4. Conclusions

An experimental investigation was performed on the effects of coupling internal/external EGR and split injection on knock suppression and combustion characteristics in a natural aspirated single-cylinder GDI engine. The results can be summarised as follows:

(1) Experimental results of SACI combustion with i-EGR strategy indicate that the IT and i-EGR ratio are important parameters for controlling SACI combustion process. The i-EGR controls the combustion phase in SACI mode mainly by changing the initial in-cylinder temperature and intake mass flow rate. The R_{si} drops as the i-EGR ratio increases. Similar to the traditional SI mode, the combustion phase is controlled by adjusting the IT in SACI mode. When the IT is excessively advanced, the excessive R_{ci} leads to knocking combustion. When the IT is excessively delayed, the basic heat release process is similar to that of the SI combustion and misfire cycles occasionally appear.

(2) The i & e-EGR strategy can effectively suppress knock in SACI mode. With an increase in e-EGR ratio, MAPO decreases significantly and its probability distribution becomes more concentrated. The effects of e-EGR on knocking suppression are generally achieved by decreasing the in-cylinder temperature, diluting the fuel/air mixture and increasing the heat capacity, which result in longer ignition delay time, lower R_{ci} value and lower knock intensity. In addition, the engine performance with i & e-EGR strategy can be improved by more advancing IT and less negative work during NVO period compared to the only i-EGR strategy.

(3) The i-EGR & Split strategy has a significant impact on knock suppression. The effect of split injection on knock suppression demonstrates the non-monotonic relationship at different levels of fuel stratification. The effect of the split injection strategy on knock suppression is also influenced by the initial in-cylinder temperature. When initial in-cylinder temperature is high with large i-EGR ratio, the knock propensity first decreases and then increases as the SOI_2 is gradually retarded. However, when the i-EGR ratio is as low as 6.9%, which obtains a low initial in-cylinder temperature, the knock suppression effect of split injection increases monotonically with the delay of SOI_2.

(4) The EGR & Split strategy combines the advantages of both split injection and e-EGR, allowing the best knock resistance to be obtained. In addition, the coupling strategy that combines internal/external EGR and split injection demonstrates the best engine performance, with BMEP increasing approximately 0.1 MPa and BSFC decreasing by approximately 27 g/kW•h relative to the baseline case.

Acknowledgments

This work is supported by National Natural Science Foundation of China (Grant No.91641203,51606133).We also thank to the support of National Key R&D Program of China.

Nomenclature

SI	Spark Ignition	MBT	Minimum spark advance for Best Torque
CI	Compression Ignition	MAPO	Maximum Amplitude of filtered Pressure Oscillation
HCCI	Homogeneous Charge Compression Ignition	EGR	Exhaust Gas Recirculation
SACI	Spark Assisted Compression Ignition	PLIF	Planar Laser Induced Fluorescence
PPC	Partially Premixed Compression	VVT	Variable Valve Timing
GDI	Gasoline Direct Inject	η	Brake thermal efficiency
CAD	Crank Angle Degree	λ	Equivalence ratio
BTDC	Before Top Dead Center	γ	Ratio of specific heats
NVO	Negative Valve Overlap	IMEP	Indicate Mean Effective Pressure
IT	Ignition Timing	BMEP	Brake Mean Effective Pressure
R_{ci}	Ratio of CI heat release	BSFC	Brake Specific Fuel Consumption
R_{si}	Ratio of SI heat release	CR	Compression Ratio
ROI	Ratio of Inject	WOT	Widely Open Throttle
SOI	Start of Inject	EVC	Exhaust Valve Closing
P_{max}	Maximum Pressure	EVO	Exhaust Valve Opening
HRR	Heat Release Rate	IVC	Intake Valve closing
MFB	Mass Fraction Burned	IVO	Intake Valve closing

References

[1] H. Bendu, S. Murugan, Homogeneous charge compression ignition (HCCI) combustion: Mixture preparation and control strategies in diesel engines, Renewable Sustainable Energy Rev 38 (2014) 732-746.

[2] X.-C. Lü, W. Chen, Z. Huang, A fundamental study on the control of the HCCI combustion and emissions by fuel design concept combined with controllable EGR. Part 2. Effect of operating conditions and EGR on HCCI combustion, Fuel 84 (2005) 1084-1092.

[3] A.P. Singh, A.K. Agarwal, Combustion characteristics of diesel HCCI engine: An experimental investigation using external mixture formation technique, Appl. Energy 99 (2012) 116-125.

[4] M. Sjöberg, J.E. Dec, Comparing late-cycle autoignition stability for single- and two-stage ignition fuels in HCCI engines, Proc. Combust. Inst. 31 (2007) 2895-2902.

[5] Y. Yang, J.E. Dec, N. Dronniou, M. Sjöberg, Tailoring HCCI heat-release rates with partial fuel stratification: Comparison of two-stage and single-stage-ignition fuels, Proc. Combust. Inst. 33 (2011) 3047-3055.

[6] M. Canakci, An experimental study for the effects of boost pressure on the performance and exhaust emissions of a DI-HCCI gasoline engine, Fuel 87 (2008) 1503-1514.

[7] J. Hunicz, A. Tmar, P. Krzaczek, Effects of Mixture Stratification on Combustion and Emissions of Boosted Controlled Auto-Ignition Engines, Energies 10 (2017) 2172.

[8] Z. Wang, X. He, J.-X. Wang, S. Shuai, F. Xu, D. Yang, Combustion visualization and experimental study on spark induced compression ignition (SICI) in gasoline HCCI engines, Energy Convers. Manage. 51 (2010) 908-917.

[9] R.J. Middleton, L.K.M. Olesky, G.A. Lavoie, M.S. Wooldridge, D.N. Assanis, J.B. Martz, The effect of spark timing and negative valve overlap on Spark Assisted Compression Ignition combustion heat release rate, Proc. Combust. Inst. 35 (2015) 3117-3124.

[10] L.M. Olesky, J.B. Martz, G.A. Lavoie, J. Vavra, D.N. Assanis, A. Babajimopoulos, The effects of spark timing, unburned gas temperature, and negative valve overlap on the rates of stoichiometric spark assisted compression ignition combustion, Appl. Energy 105 (2013)

407-417.

[11] X. Wang, H. Xie, L. Li, L. Xie, T. Chen, H. Zhao, Wall temperature effect on SI-CAI hybrid combustion progress in a gasoline engine, SAE Pap. (2013), 2013-01-1662.

[12] L. Koopmans, I. Denbratt, A four stroke camless engine, operated in Homogeneous Charge Compression Ignition mode with commercial gasoline, SAE Pap. (2001), 2001-01-3610.

[13] S.M. Begg, D.J. Mason, M.R. Heikal, Spark ignition and spark-assisted controlled auto-ignition in an optical gasoline engine, SAE Pap. (2009), 2009-32-0072.

[14] C.S. Yoo, Z. Luo, T. Lu, H. Kim, J.H. Chen, A DNS study of ignition characteristics of a lean iso-octane/air mixture under HCCI and SACI conditions, Proc. Combust. Inst. 34 (2013) 2985-2993.

[15] W.J. Glewen, R.M. Wagner, K.D. Edwards, C.S. Daw, Analysis of cyclic variability in spark-assisted HCCI combustion using a double Wiebe function, Proc. Combust. Inst. 32 (2009) 2885-2892.

[16] J. Benajes, A. García, V. Domenech, R. Durrett, An investigation of partially premixed compression ignition combustion using gasoline and spark assistance, Appl. Therm. Eng. 52 (2013) 468-477.

[17] Z. Wang, J. Wang, S. Shuai, X. He, F. Xu, D. Yang, X. Ma, Research on spark induced compression ignition (SICI), SAE Pap. (2009), 2009-01-0132.

[18] J.V. Pastor, J.M. García-Oliver, A. García, C. Micó, R. Durrett, A spectroscopy study of gasoline partially premixed compression ignition spark assisted combustion, Appl. Energy 104

(2013) 568-575.

[19] J. Benajes, B. Tormos, A. Garcia, J. Monsalve-Serrano, Impact of spark assistance and multiple injections on gasoline PPC light load, SAE Pap. 7 (2014) 1875-1887.

[20] G.A. Lavoie, J. Martz, M. Wooldridge, D. Assanis, A multi-mode combustion diagram for spark assisted compression ignition, Combust. Flame 157 (2010) 1106-1110.

[21] H. Xie, L. Li, T. Chen, W. Yu, X. Wang, H. Zhao, Study on spark assisted compression ignition (SACI) combustion with positive valve overlap at medium–high load, Appl. Energy 101 (2013) 622-633.

[22] L.M. Olesky, G.A. Lavoie, D.N. Assanis, M.S. Wooldridge, J.B. Martz, The effects of diluent composition on the rates of HCCI and spark assisted compression ignition combustion, Appl. Energy 124 (2014) 186-198.

[23] L. Manofsky, J. Vavra, D.N. Assanis, A. Babajimopoulos, Bridging the gap between HCCI and SI: Spark-Assisted Compression Ignition, SAE Pap. (2011), 2011-01-1179.

[24] X. Wang, H. Xie, L. Li, L. Xie, T. Chen, H. Zhao, Effect of the thermal stratification on SI–CAI hybrid combustion in a gasoline engine, Appl. Therm. Eng. 61 (2013) 451-460.

[25] D. Li, Z. Wang, H. Liu, J.X. Wang, Combustion Mode Switch by Integrating Stoichiometric ASSCI Mode in a Four-cylinder Gasoline SI/HCCI Engine, SAE Pap. (2014), 2014-01-1288.

[26] H. Persson, J. Sjöholm, E. Kristensson, B. Johansson, M. Richter, M. Aldén, Study of fuel stratification on Spark Assisted Compression Ignition (SACI) combustion with ethanol using high speed fuel PLIF, SAE Pap. (2008), 2008-01-2401.

[27] J. Benajes, S. Molina, A. García, J. Monsalve-Serrano, R. Durrett, Performance and engine-out emissions evaluation of the double injection strategy applied to the gasoline partially premixed compression ignition spark assisted combustion concept, Appl. Energy 134 (2014) 90-101.

[28] G. Marseglia, M. Costa, F. Catapano, P. Sementa, B.M. Vaglieco, Study about the link between injection strategy and knock onset in an optically accessible multi-cylinder GDI engine, Energy Convers. Manage. 134 (2017) 1-19.

[29] M. Pan, G. Shu, H. Wei, T. Zhu, Y. Liang, C. Liu, Effects of EGR, compression ratio and boost pressure on cyclic variation of PFI gasoline engine at WOT operation, Appl. Therm. Eng. 64 (2014) 491-498.

[30] D. Feng, H. Wei, M. Pan, Comparative study on combined effects of cooled EGR with intake boosting and variable compression ratios on combustion and emissions improvement in a SI engine, Appl. Therm. Eng. 131 (2018) 192-200.

[31] E.A. Ortiz-Soto, J. Vavra, A. Babajimopoulos, Assessment of residual mass estimation methods for cylinder pressure heat release analysis of HCCI Engines with negative valve overlap, J. Eng. Gas Turbines Power 134 (2012) 082802.

[32] R.G. Prucka, Z. Filipi, D.N. Assanis, D.M. Kramer, G.L. Ohl, An evaluation of residual gas fraction measurement techniques in a high degree of freedom spark ignition engine, SAE Pap. 1 (2008) 71-84.

[33] E. Galloni, Dynamic knock detection and quantification in a spark ignition engine by means of a pressure based method, Energy Convers. Manage. 64 (2012) 256-262.

[34] G. Brecq, J. Bellettre, M. Tazerout, A new indicator for knock detection in gas SI engines, International Journal of Thermal Sciences 42 (2003) 523-532.

[35] G. Shu, J. Pan, H. Wei, Analysis of onset and severity of knock in SI engine based on in-cylinder pressure oscillations, Appl. Therm. Eng. 51 (2013) 1297-1306.

[36] Y. Liu, X. Shi, J. Deng, Y. Chen, M. Hu, L. Li, Experimental study on the characteristics of knock under DI-HCCI combustion mode with ethanol/gasoline mixed fuel, SAE Pap. (2013), 2013-01-0544.

[37] U. Azimov, N. Kawahara, E. Tomita, UV–visible light absorption by hydroxyl and formaldehyde and knocking combustion in a DME-HCCI engine, Fuel 98 (2012) 164-175.

[38] L. Zhou, J. Hua, H. Wei, K. Dong, D. Feng, G. Shu, Knock characteristics and combustion regime diagrams of multiple combustion modes based on experimental investigations, Appl. Energy 229 (2018) 31-41.

[39] Heywood, JohnB, Internal combustion engine fundamentals, McGraw-Hill, 1988.

[40] C.D. Rakopoulos, C.N. Michos, E.G. Giakoumis, Availability analysis of a syngas fueled spark ignition engine using a multi-zone combustion model, Energy 33 (2008) 1378-1398.

[41] Z. Wang, J.X. Wang, S.J. Shuai, Q.J. Ma, New gasoline homogeneous charge compression ignition combustion system using two-state direct injection and assisted spark ignition, Proc. Inst. Mech. Eng. 220 (2006) 367-378.

[42] L. Cao, H. Zhao*, X. Jiang, Analysis of Controlled Auto-Ignition/HCCI Combustion in a Direct Injection Gasoline Engine with Single and Split Fuel Injections, Combust. Sci. Technol 180 (2007) 176-205.